IIETA International Information and Engineering Technology Association
Advancing the World of Information and Engineering

Traitement du Signal
Vol. 41, No. 4, August, 2024, pp. 1797-1805
Journal homepage: http://iieta.org/journals/ts

Adaptive Signal Filtering and Health Monitoring for Electric Motor Control Systems in New Energy Vehicles

Lei Yu

Changchun Information Technology Vocational College, Changchun 130000, China

Corresponding Author Email: masen2013@163.com

https://doi.org/10.18280/ts.410412

Received: 3 March 2024
Revised: 20 June 2024
Accepted: 11 July 2024
Available online: 31 August 2024

Keywords:
new energy vehicles, electric motor control systems, health monitoring, adaptive signal filtering, magnetic flux estimation, hierarchical transfer learning

ABSTRACT

With the widespread adoption of new energy vehicles and the push for environmental policies, the performance and reliability of electric motors, a core component of these vehicles, have become increasingly important. Effective health monitoring of electric motor control systems not only enhances operational efficiency but also extends the motor's lifespan and reduces maintenance costs. Thus, accurately monitoring motor performance and diagnosing faults in a timely manner has become a focal point of current research. However, existing methods show instability under complex operating conditions and suffer from inaccuracies in signal filtering and fault detection. To address these issues, this paper proposes an adaptive signal filtering method based on Extended Kalman Filtering (EKF) combined with magnetic flux estimation and hierarchical transfer learning strategies for health monitoring, aiming to improve model generalization and detection performance. This research provides new technological support for the health monitoring of electric motor control systems in new energy vehicles, offering significant theoretical and practical value.

1. INTRODUCTION

With the increasing global awareness of environmental protection and the promotion of energy-saving and emission-reduction policies, new energy vehicles, as a green travel option, have received more and more attention and support [1-3]. As the core component of new energy vehicles, the performance and reliability of electric motors directly affect the overall operation and lifespan of the vehicle [4, 5]. Therefore, effective health monitoring of the electric motor control system in new energy vehicles, timely detection and handling of potential faults, has become an important research topic to ensure the safe operation of new energy vehicles.

Research shows that health monitoring of the electric motor control system in new energy vehicles not only helps to improve the operating efficiency of the motor but also effectively reduces maintenance costs and extends the equipment's service life [6-10]. Therefore, conducting research on health monitoring for the electric motor control system in new energy vehicles has significant theoretical and practical importance. By deeply analyzing the motor's operating state, timely warning and diagnosing faults can significantly enhance the safety and reliability of new energy vehicles, promoting the sustainable development of the new energy vehicle industry.

However, existing health monitoring methods and technologies still have some shortcomings in practical applications [11-15]. For example, traditional signal filtering and fault diagnosis methods struggle to achieve satisfactory results under complex and variable operating conditions, easily being affected by noise and interference [16, 17]. In addition, current transfer learning strategies, when applied to model training, may lead to underfitting or overfitting problems due to improper selection of frozen layers, affecting detection performance [18-20]. Therefore, there is an urgent need for an advanced method that can adapt to the complex operating conditions of new energy vehicle motors to improve the accuracy and stability of signal filtering and fault detection.

This paper includes two parts: one is the adaptive signal filtering and magnetic flux estimation for the electric motor control system in new energy vehicles, and the other is the health monitoring for the electric motor control system in new energy vehicles. In terms of adaptive signal filtering and magnetic flux estimation, this paper proposes a method based on EKF to improve the estimation accuracy of magnetic flux parameters and the control performance of the system. In terms of health monitoring, this paper introduces a hierarchical transfer learning strategy to improve the model's generalization ability and detection performance by progressively freezing and fine-tuning network layers. The research in this paper not only provides new ideas and methods for health monitoring of the electric motor control system in new energy vehicles but also has significant theoretical and practical value.

2. ADAPTIVE SIGNAL FILTERING AND FLUX ESTIMATION FOR ELECTRIC MOTOR CONTROL IN NEW ENERGY VEHICLES

In the electric motor control system of new energy vehicles, accurate magnetic flux estimation is one of the key factors for

achieving efficient and stable control. Traditional magnetic flux estimation methods often fail to provide sufficient accuracy and robustness when faced with changes in motor parameters and measurement noise. This paper introduces EKF as a solution, mainly because EKF can effectively handle state estimation problems in nonlinear systems and has strong adaptive capabilities. EKF is based on Kalman Filtering and extends to nonlinear systems by linearizing nonlinear equations and recursively updating the state estimates and their covariance, making it suitable for the nonlinear characteristics of motors. Moreover, load changes, parameter drift, and sensor noise that may occur during motor operation can significantly affect the accuracy of magnetic flux estimation. EKF can dynamically adjust filtering parameters by real-time updating of system state predictions and observation information, reducing the interference of noise on the system, thereby improving estimation accuracy.

In new energy vehicle motors, the magnitude and direction of the magnetic flux vector have a direct impact on the motor's operating state. Changes in the magnetic flux vector can reflect whether the motor has faults and the specific location and nature of the faults. For example, a sudden change in magnetic flux magnitude may indicate an internal short circuit or open circuit in the motor, while an abnormal magnetic flux direction may indicate problems such as stator or rotor imbalance. By analyzing the magnetic flux vector, faults can be detected and diagnosed in a timely manner to ensure normal motor operation. The *d-q* axis positioning converts the three-phase AC *abc* coordinate system into the DC *d-q* coordinate system, which simplifies the motor's control algorithm and improves control accuracy and response speed. The *d-q* axis voltage equations are the foundation of the motor's mathematical model, describing the voltage and current relationships in the *d-q* coordinate system. The purpose of constructing these equations is to provide an accurate mathematical model for subsequent magnetic flux estimation. By establishing the voltage equations, the dynamic behavior of the motor can be clearly understood, providing necessary input data for control algorithms.

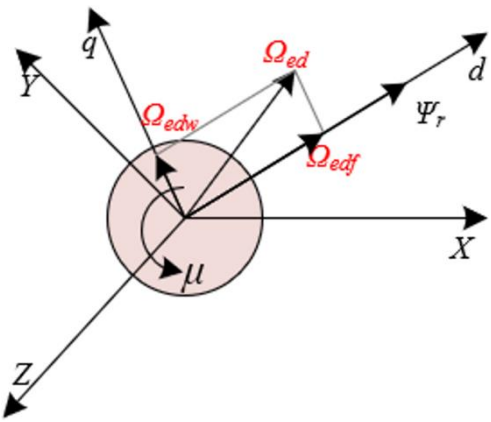

Figure 1. Changes in magnetic flux of electric motor in new energy vehicles

Figure 1 shows a schematic of changes in magnetic flux of the electric motor in new energy vehicles. Specifically, when a fault occurs, the *d-q* axis positioning of the system changes, and the initial magnetic flux Ω_e becomes Ω_{ed}. Ω_{ed} will produce new mappings Ω_{edf} and Ω_{edw} on the *d-q* axis. The original *d-q* axis voltage equations will change to:

$$\begin{cases} u_f = Ei_f + M\dfrac{di_f}{ds} - \mu M i_w - \mu\Omega_{ew} \\ u_w = Ei_w + M\dfrac{di_w}{ds} - \mu M i_w - \mu\Omega_{ef} \end{cases} \tag{1}$$

To improve the accuracy of magnetic flux estimation, magnetic flux parameters need to be introduced as observation quantities into EKF. By using EKF to update and correct magnetic flux parameters in real-time, the estimation can more accurately reflect the actual operating state of the motor. The specific implementation process includes rewriting the original *d-q* axis voltage equations and introducing the state estimation and covariance update steps of EKF. The rewritten equations are:

$$\begin{cases} \dfrac{di_f}{ds} = \dfrac{u_f}{M} - \dfrac{E}{M}i_f + \mu i_f + \mu\dfrac{\Omega_{ew}}{M} \\ \dfrac{di_w}{ds} = \dfrac{u_w}{M} - \dfrac{E}{M}i_w + \mu i_f + \mu\dfrac{\Omega_{ef}}{M} \end{cases} \tag{2}$$

Under steady-state operating conditions of the electric motor in new energy vehicles, changes in the *d-q* axis magnetic flux are relatively small and can generally be considered as steady-state values. This is because during stable operation, parameters such as motor current, voltage, and speed do not fluctuate dramatically, and the magnetic flux tends toward a stable value. This assumption simplifies the calculation process for magnetic flux estimation, helping to improve filtering efficiency and real-time performance. At this time, there is:

$$\begin{cases} d\Omega_{ef}/ds = 0 \\ d\Omega_{ew}/ds = 0 \end{cases} \tag{3}$$

The nonlinear system model of the new energy vehicle motor includes the motor's electromagnetic and mechanical dynamic equations, which describe the relationships between voltage, current, torque, and speed. These models are highly nonlinear because they involve complex electromagnetic phenomena and mechanical motion within the motor. To apply them in a digital control system, these nonlinear equations need to be discretized. Let the system noise be represented by $\delta(s)$, measurement noise by $\omega(s)$, and their variance matrices by $W(s)$ and E, the input quantity by $i(s)$, state vector by $a(s)$, and output quantity by $b(s)$. According to the definition of EKF, the nonlinear system model of the new energy motor and its discretized nonlinear measurement equations can be listed as:

$$\begin{cases} a(s) = \Gamma[a(s)] + Yi(s) + \delta(s) \\ b(s_j) = g[a(s)] + \omega(s_j) \end{cases} \tag{4}$$

Further mathematical expressions for the state vector, input quantity, and output quantity are constructed. The state vector typically includes key state parameters of the system, such as magnetic flux, current, and speed. The input quantity includes the voltage applied by the control system and external load torque. The output quantity is measurable parameters of the system, such as current and voltage. Specifically, according to the physical model and control objectives of the motor, these

quantities are defined mathematically and incorporated into the EKF framework:

$$\begin{cases} a=\left[u_f \quad u_w \quad \Omega_{ef} \quad \Omega_{ew}\right]^S \\ i=\left[i_f/M \quad i_w/M\right]^S \\ b=\left[u_f \quad u_w\right]^S \end{cases} \tag{5}$$

The *Jacobian* matrix is:

$$D\left[a(s)\right]=\left.\frac{d\Gamma}{da}\right|_{a=a(s)}=\begin{bmatrix} -\frac{E}{M} & \mu & 0 & \frac{\mu}{M} \\ -\mu & -\frac{E}{M} & -\frac{\mu}{M} & 0 \\ 0 & 0 & 0 & 0 \\ 0 & 0 & 0 & 0 \end{bmatrix} \tag{6}$$

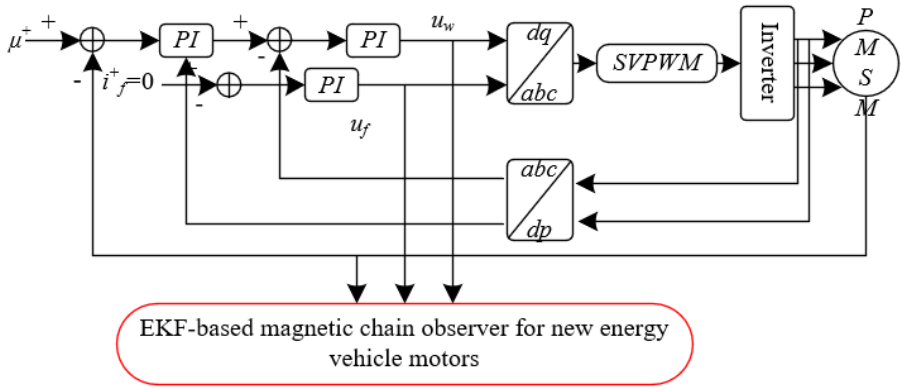

Figure 2. EKF magnetic flux estimation principal diagram

Figure 2 shows the principal diagram of EKF for magnetic flux estimation. EKF is mainly divided into two stages: the prediction stage and the correction stage. In the prediction stage, the system's nonlinear model is used to predict the state value and covariance matrix for the next time step. This step calculates the future state using the system's state transition equations and estimates system uncertainty. This stage is represented by Eq. (7). In the correction stage, the predicted values are adjusted using actual measurement values, updating the state estimate and covariance matrix. This step uses the measurement equations and actual measured data to feedback prediction errors into the state estimate, correcting the prediction results. This stage is represented by Eq. (8). The specific implementation process includes performing prediction and correction operations at each time step, iteratively improving the accuracy of magnetic flux parameter estimation. Let the sampling time interval be represented by S, then:

$$\begin{cases} a_{rj|j-1}=a_{rj-1|j-1}+\left[\Gamma\left(a_{rj-1|j-1}\right)+Y\left\langle i_{j-1}\right\rangle\right]S_z \\ O_{j|j-1}=O_{j-1|j-1}+\left(D_{j-1}O_{j-1|j-1}+O_{j-1|j-1}D'_{j-1}\right)S_z+W_f \end{cases} \tag{7}$$

where,

$$D_{j-1}=\left.\frac{\partial\Gamma(a)}{\partial a}\right|_{a=a_{rj-1|j-1}} \tag{8}$$

In practical system applications, the system noise covariance matrix typically includes a combination of a diagonal matrix, a time-varying matrix, and a non-time-varying matrix. However, due to time and computational resource constraints, it can be simplified to use a non-time-varying diagonal matrix instead. This simplification significantly reduces computational complexity while maintaining estimation accuracy, allowing EKF to operate efficiently in real-time systems. The specific implementation involves selecting appropriate diagonal element values representing the variance of system noise and using this simplified matrix in the EKF update steps. Let the Kalman filter coefficient matrix be represented by J_j, then:

$$\begin{cases} a_{rj|j}=a_{rj|j-1}+J_j\left[b_j-g\left(a_{rj|j-1}\right)\right] \\ O_{j|j}=O_{j|j-1}-J_jG_jO_{j|j-1} \end{cases} \tag{9}$$

where,

$$\begin{cases} J_j=O_{j|j-1}G'_j\left(GO_{j|j-1}G'_j+E\right)^{-1} \\ G_j=\partial g(a)/\partial a\left|_{a=a_{rj|j-1}}\right. \end{cases} \tag{10}$$

3. HEALTH MONITORING OF ELECTRIC MOTOR CONTROL SYSTEMS IN NEW ENERGY VEHICLES

During operation, the electric motor control system in new energy vehicles is prone to anomalies due to various factors, such as component aging and changes in external environment. Timely and accurate anomaly detection is crucial for ensuring system stability and safety. However, traditional model training methods often fail to achieve satisfactory detection results in the face of complex and variable real-world conditions. To address this issue, this paper proposes using a hierarchical transfer learning approach to enhance the model's generalization ability and detection performance.

Traditional transfer learning strategies involve freezing some network layers to retain knowledge learned from previous tasks and fine-tuning the model based on this retained knowledge. However, this method encounters challenges in choosing the number of layers to freeze. Too many frozen layers may lead to underfitting in the new task, making it

difficult to capture new features; whereas too few frozen layers may result in insufficient utilization of the knowledge accumulated from previous tasks, leading to poor model performance. To find a balance between these extremes, this paper introduces a hierarchical transfer learning strategy, which involves gradually freezing and fine-tuning network layers, allowing the model to fully utilize historical knowledge and adapt to new task characteristics.

The specific implementation of hierarchical transfer learning includes: first, based on the training results from previous tasks, dividing the network layers into several levels and progressively freezing the network layers according to these levels; then, fine-tuning at each level to enable the model to retain historical knowledge while flexibly adapting to new task requirements. This hierarchical approach helps avoid the issues caused by improper layer selection in traditional methods, thus improving the model's robustness and detection performance.

3.1 Sample hierarchical strategy

Figure 3 shows the hierarchy of samples for health monitoring of the electric motor control system in new energy vehicles. Assume that each model training is an independent task set X, where X includes the previous task set $X_{OL}=\{S_1,...,S_u\}$ and the new task $X_{NE}=\{S_{u+1}\}$. The dataset D used for each model training is similarly divided into the previous task dataset set $F_{OL}=\{a^e_1,...,a^e_u\}$ and the new dataset set $F_{NE}=\{a^e_{u+1}\}$. The hierarchical transfer strategy proposed in this paper first sorts the mixed data hierarchically, dividing it into three sets based on the complexity of the data: $F_{JD}=\{a^e_1,...,a^e_u,a^e_{u+1}\}$, $F_{ZD}=\{a^e_1,...,a^e_u,a^e_{u+1}\}$, and $F_{KN}=\{a^e_1,...,a^e_u,a^e_{u+1}\}$. In practical applications, for health monitoring of the electric motor control system in new energy vehicles, the F_{JD} set may include common and easily identifiable fault pattern data; the F_{ZD} set may contain moderately complex fault pattern data; and the F_{KN} set may include extremely complex or rare fault pattern data. By using this hierarchical training method, the model can progressively learn and adapt to fault data of varying complexities at different stages, thereby effectively enhancing its ability to recognize and detect complex fault patterns.

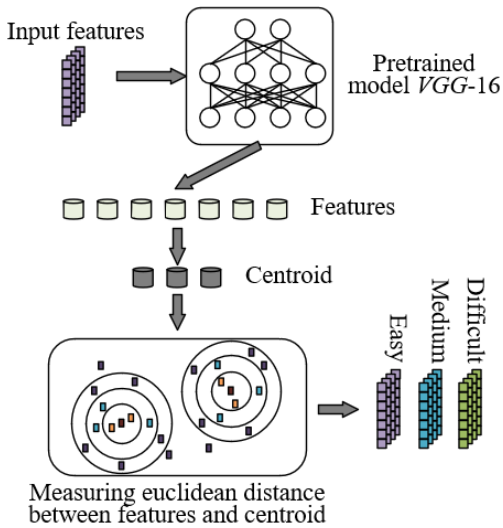

Figure 3. Hierarchical classification of health monitoring samples for electric motor control systems in new energy vehicles

In the research on health monitoring of electric motor control systems for new energy vehicles, two key issues must be addressed to implement the hierarchical transfer training strategy proposed in this paper. 1) An effective method for measuring hierarchical difficulty needs to be designed to sort mixed data from easy to difficult. To achieve this, a systematic approach is used to assess the classification difficulty of each sample. This involves analyzing the feature complexity of the sample, the prominence of fault modes, and the recognition difficulty in historical data to grade each sample's difficulty. 2) An effective model training process needs to be designed to guide the model to learn from the classified mixed data sequentially. For health monitoring of electric motor control systems in new energy vehicles, the training process should start with simple samples and gradually introduce more complex samples, enabling the model to progressively adapt to and learn from fault data of varying complexities.

To this end, this paper proposes a hierarchical training strategy based on image datasets to improve the model's detection accuracy and robustness. The specific training strategy includes the following steps:

(1) Selecting a pre-trained model: First, choose a pre-trained model to extract features from the samples. In this paper, the classic VGG-16 model is used as the pre-trained model for experimentation. In health monitoring of electric motor control systems, the motor's operating state can be converted into image form through various sensor data, and VGG-16 is used to extract feature information from these images, providing a basis for subsequent sample classification and grading.

(2) Inputting mixed samples: Input the mixed samples into the trained pre-trained model to project all samples into the same feature space. In the health monitoring of motor control systems, these samples may include image data from normal operating conditions and various fault modes. Through this process, each sample is converted into a 2048-dimensional vector, which will be used in subsequent steps to assess the difficulty of sample classification.

(3) Collecting feature centroids: Collect a set of feature centroids for normal motor types and abnormal motor types, respectively. By calculating the Euclidean distance between samples and these centroids, the difficulty of classifying each sample is determined. If the distance of a sample to the nearest centroid is below a predefined threshold, update the value of that centroid; if the distance is above the threshold, create a new centroid and set it equal to the vector of the sample.

(4) Dividing into subsets: Based on the Euclidean distance from sample vectors to their nearest feature centroids, divide the samples into three subsets. Simple samples are those closest to the centroids, while others are more distant. Specifically, simple samples F_{JD} are those with a short distance to the centroids; moderately difficult samples F_{ZD} have a moderate distance; and difficult samples F_{KN} are those with a longer distance. In health monitoring of motor control systems, this means grading samples based on the complexity of fault features, which helps the model gradually adapt to different complexities of fault modes.

Specifically, assume that the iu-th anomaly detection task is represented by u, and the sample index is represented by o. Input each sample $a_{u,o}$ from the anomaly detection task S into the pre-trained neural network model Γ to obtain its sample vector $n_{u,o}$:

$$n_{u,o}=\Gamma\left(a_{u,o}\right) \tag{11}$$

Assume that the total dimension of the feature vector is v, the sample vector index is o, the centroid index is w, the computed Euclidean distance is j, the sample vector is n, and the centroid set is zn. The formula for calculating the nearest centroid is:

$$j_{o,w}^{u} = \sqrt{\sum_{m=1}^{v} \left(n_{u,o} - zn_{u,w} \right)^2} \tag{12}$$

Assume that the number of existing samples within the threshold range around the centroid is V. If the distance of the sample vector to the nearest centroid is less than the set threshold, it should be updated according to the following formula:

$$zn_{u,w}^{NE} = \frac{V * zn_{u,w} + n_{u,o}}{V + 1} \tag{13}$$

If the distance is greater than the threshold, a new centroid will be added based on the following equation:

$$zn_{u,w+1} = n_{u,o} \tag{14}$$

Finally, based on the rule that shorter Euclidean distances indicate simpler samples, arrange the samples in order from simple to complex. In the same feature space, subsets closer to the feature centroids are defined as clean data $\{a_u\}^{JD}$, while subsets farther from the feature centroids are defined as complex data $\{a_u\}^{KN}$. By arranging subsets from simple to complex, i.e., in increasing order of classification difficulty, the model can be gradually guided to learn. For health monitoring of electric motor control systems in new energy vehicles, this gradual guidance method enables the model to learn from simple fault modes and progressively adapt to and master complex fault modes, thereby improving detection accuracy and robustness.

3.2 Hierarchical transfer process

The hierarchical transfer process is as follows: First, according to the sample classification strategy, the current task's normal sample types and abnormal sample types are divided into simple datasets containing images of normal operating states and minor fault modes, moderate datasets containing more complex fault modes, and difficult datasets containing the most complex and rare fault modes. If the current task is not the first task, part of the dataset from previous tasks with the same difficulty level will also be added to these three datasets. The purpose of adding previous sample data is to prevent forgetting past knowledge and ensure that the model retains and applies the knowledge learned previously when handling new tasks. Furthermore, the pre-trained model needs to be loaded. In this paper, the CAT model, which includes Convolutional Neural Network (CNN), Self-Attention mechanism, and Temporal Convolutional Network (TCN) layers, is used as the pre-trained model for further experimentation.

The difficult dataset is input into the CAT model with the CNN model and Self-Attention model frozen for training. The purpose of freezing the model is to fix the lower-layer feature extraction part and focus on fine-tuning the higher-layer features, thus improving the model's robustness when handling complex data. The moderate and difficult datasets are input into the CAT model with the CNN model, Self-Attention model, and one layer of TCN model frozen for training. By introducing the TCN layer, better temporal information capture is achieved, which helps enhance the model's ability to identify fault modes in the motor control system.

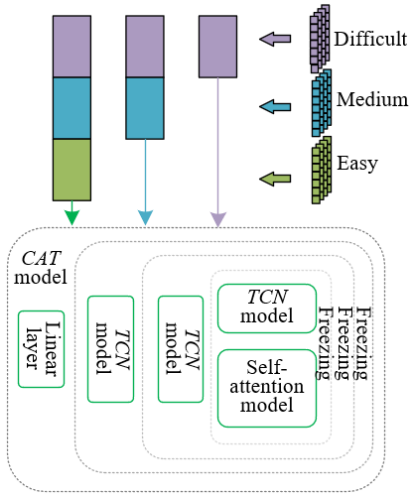

Figure 4. Hierarchical transfer-based health monitoring process for new energy vehicle motor control systems

Finally, all training set data are input into the CAT model with the CNN model, Self-Attention model, and two layers of TCN model frozen for training. At this point, the model can handle a range of data from simple to complex and can fully utilize temporal information for fault detection. After training, the final model weights for abnormal detection in new energy vehicle motors can be obtained. Figure 4 shows the hierarchical transfer-based health monitoring process for new energy vehicle motor control systems.

4. EXPERIMENTAL RESULTS AND ANALYSIS

Table 1. Simulation results for adaptive filtering and flux identification in new energy vehicle motors

Magnetic Flux Setpoint (Wb)	Magnetic Flux Identification Value (Wb)	Absolute Error (Wb)	Relative Error
0.3325	0.3324	-0.0014	0.43%
0.3214	0.3256	0.0032	1.00%
0.3125	0.3268	0.0041	1.32%
0.3069	0.3021	-0.0008	0.25%
0.2895	0.2898	0.0011	0.42%

Table 1 presents detailed data from the adaptive signal filtering magnetic flux identification simulation results for new energy vehicle motor control systems. Specifically, the magnetic flux setpoint values range from 0.2895 Wb to 0.3325 Wb. The identification results show that the absolute error between the magnetic flux identification value and the setpoint ranges from -0.0014 Wb to 0.0041 Wb, while the relative error ranges from 0.25% to 1.32%. The highest relative error is observed when the magnetic flux setpoint is 0.3125 Wb, reaching 1.32%, and the smallest relative error is observed when the magnetic flux setpoint is 0.3069 Wb, at only 0.25%. Overall, the magnetic flux identification results show relatively small errors compared to the setpoint values, indicating that the adaptive signal filtering method used has

high precision in magnetic flux parameter identification. From the data in the table, it can be concluded that the EKF method performs well in adaptive signal filtering magnetic flux identification for new energy vehicle motor control systems. Although there are some absolute and relative errors, these errors are within an acceptable range, suggesting that the method effectively estimates magnetic flux parameters. The particularly small relative error further demonstrates the robustness and accuracy of the method.

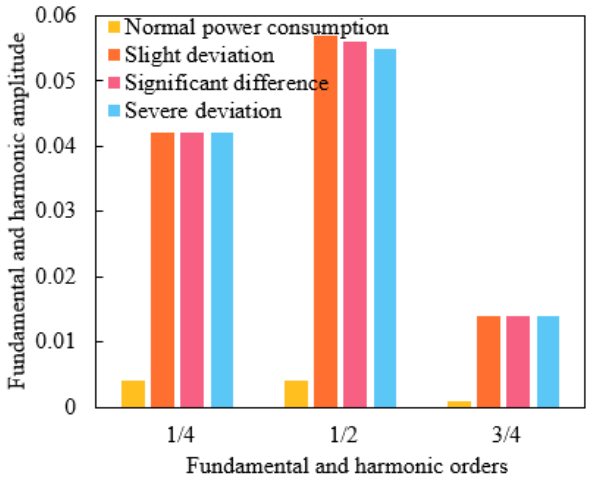

Figure 5. Current harmonic analysis based on magnetic flux identification

Figure 5 displays the current harmonic analysis results of the new energy vehicle motor control system under fundamental and harmonic conditions, corresponding to four states: normal power consumption, slight deviation, significant anomaly, and severe deviation. At a fundamental/harmonic order of 1/4, the normal power consumption value is 0.004, while for slight deviation, significant anomaly, and severe deviation, the power consumption values are all 0.042. At a fundamental/harmonic order of 1/2, the normal power consumption remains 0.004, while for slight deviation, significant anomaly, and severe deviation, the power consumption values are 0.057, 0.056, and 0.055, respectively. At a fundamental/harmonic order of 3/4, the normal power consumption value is the lowest at 0.001, while the power consumption values for the other three states are closer, at 0.014 each. From the data in the figure, it is observed that as the fundamental/harmonic order increases, the normal power consumption is significantly lower than that under abnormal conditions, indicating that the motor control system under normal operation has fewer harmonic components in the current and lower energy loss. In the cases of slight deviation, significant anomaly, and severe deviation, the power consumption values do not change much with the harmonic order, particularly at fundamental/harmonic orders of 1/2 and 3/4, where the power consumption values are relatively stable but still noticeably higher than in the normal state. This result suggests that the abnormal states of the motor control system significantly increase the harmonic components in the current, leading to increased energy loss and consequently affecting the system's operational efficiency.

Figure 6 shows the current harmonic analysis results of the new energy vehicle motor control system under stable and abnormal operating conditions. At a fundamental/harmonic order of 1/4, the power consumption in the stable operating condition is 0.004, while in the abnormal operating condition, it is 0.042. At a fundamental/harmonic order of 1/2, the power consumption remains 0.004 in the stable operating condition, while in the abnormal operating condition, it is 0.047. At a fundamental/harmonic order of 3/4, the power consumption drops to 0.001 in the stable operating condition, whereas in the abnormal operating condition, it is 0.016. The data indicate that the power consumption in the abnormal operating condition is significantly higher than in the stable operating condition. From the data in Figure 6, it can be seen that the harmonic content in the current of the motor control system is significantly higher in the abnormal operating condition compared to the stable condition. Particularly at fundamental/harmonic orders of 1/4 and 1/2, the power consumption in the abnormal condition increases markedly, reaching 10 times and 11.75 times that of the stable condition, respectively. This indicates that during abnormal operation, the harmonic components in the current of the motor control system increase substantially, leading to a significant rise in energy loss and affecting the system's operational efficiency and stability. Although the increase in power consumption at a fundamental/harmonic order of 3/4 is smaller, it remains higher than in the stable condition. This suggests that current harmonic analysis can effectively distinguish between different operating states of the motor control system and verifies the effectiveness and reliability of the EKF-based adaptive signal filtering magnetic flux identification method in detecting current anomalies.

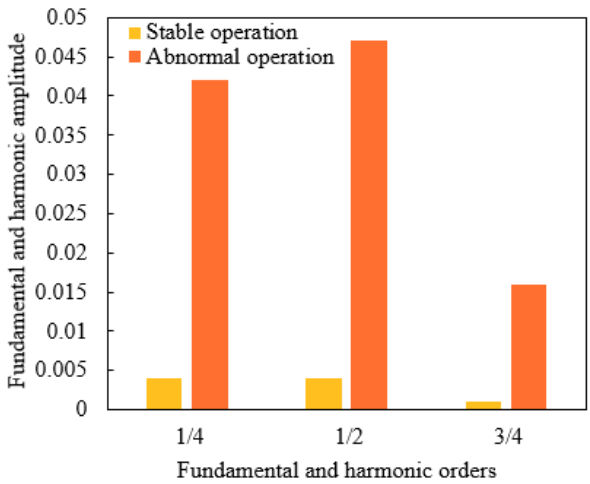

Figure 6. Current harmonic analysis based on operating conditions

Table 2 presents the criteria for health monitoring of the new energy vehicle motor control system, based on the analysis of changes in harmonics, d-axis inductance fundamental, and magnetic flux magnitude to determine the motor's health status. In Situation I and II, the motor is deemed to be in a healthy state. In Situation I, all parameters remain unchanged, while in Situation II, harmonics increase but the d-axis inductance fundamental and magnetic flux magnitude remain unchanged. Situations III and IV indicate demagnetization faults, with Situation III showing a decrease in magnetic flux magnitude and unchanged or decreased d-axis inductance fundamental, suggesting uniform demagnetization fault; Situation IV, with increased harmonics, suggests local demagnetization fault. Situations V and VI involve rotor eccentricity faults. Situation V shows increased harmonics and d-axis inductance fundamental with unchanged magnetic flux magnitude, while Situation VI indicates both

eccentricity and demagnetization faults, with all parameters showing increasing or decreasing trends. From the data in Table 2, it is evident that the patterns of change in harmonics, d-axis inductance fundamental, and magnetic flux magnitude can effectively identify different fault types in the motor. Increased harmonics are typically associated with motor faults, especially in rotor eccentricity and demagnetization faults. A decrease in magnetic flux magnitude should particularly raise the possibility of demagnetization faults, whether uniform (Situation III) or local (Situation IV). Increased d-axis inductance fundamental is often related to rotor eccentricity, particularly when eccentricity and demagnetization faults occur simultaneously (Situation VI). The introduced adaptive signal filtering and graded transfer learning strategies provide effective tools for health monitoring, enabling more precise detection of changes in motor operating conditions by progressively freezing and fine-tuning network layers, thus improving fault detection accuracy and overall system stability.

Table 2. Health monitoring criteria for new energy vehicle motor control systems

Situation Category	Harmonics	d-axis Inductance Fundamental	Magnetic Flux Magnitude	Conclusion
I	Unchanged	Unchanged	Unchanged	Motor Healthy
II	Increased	Unchanged	Unchanged	Motor Healthy
III	Unchanged	Unchanged or Decreased	Decreased	Uniform Demagnetization Fault
IV	Increased	Unchanged or Decreased	Decreased	Local Demagnetization Fault
V	Increased	Increased	Unchanged	Rotor Eccentricity Fault
VI	Increased	Increased	Decreased	Eccentricity and Demagnetization

Table 3. Experimental results of different transfer strategies

Transfer Strategy	Sample Set 1	Sample Set 2	Sample Set 3	Sample Set 4	Sample Set 5	Sample Set 6
No Pre-training	87.23%	96.54%	93.26%	98.54%	91.23%	98.57%
Frozen Fine-tuning	92.31%	98.32%	93.54%	98.62%	93.21%	98.56%
Graded Transfer	94.56%	99.36%	93.26%	98.78%	96.54%	99.32%

In the research on health monitoring of new energy vehicle motor control systems, the division and resampling of sample sets are key steps to ensure model effectiveness and robustness. This paper uses resampling techniques to extend the original sample sets, simulating conditions for multiple model retraining experiments to ensure the model's accuracy and reliability under different operating conditions and fault scenarios. Specifically, the original sample sets include four types of samples: 1000 normal samples for forward rotation, 60 abnormal samples for forward rotation, 1000 normal samples for reverse rotation, and 60 abnormal samples for reverse rotation. To extend the sample size and adapt to the graded transfer strategy, these data are resampled to generate six new sample sets. The forward rotation samples are resampled to create Sample Sets 1, 3, and 5, each containing 6000 training samples and 1500 test samples. The reverse rotation samples are resampled to create Sample Sets 2, 4, and 6, each also containing 6000 training samples and 1500 test samples.

Table 3 shows the experimental results of different transfer strategies on Sample Sets 1 to 6, including No Pre-training, Frozen Fine-tuning, and Graded Transfer strategies. The accuracy rates for the No Pre-training strategy are 87.23%, 96.54%, 93.26%, 98.54%, 91.23%, and 98.57% for Sample Sets 1 through 6, respectively. The accuracy rates for the Frozen Fine-tuning strategy are higher, at 92.31%, 98.32%, 93.54%, 98.62%, 93.21%, and 98.56%. The Graded Transfer strategy performs the best, with accuracy rates higher than the other two strategies in all sample sets, at 94.56%, 99.36%, 93.26%, 98.78%, 96.54%, and 99.32%. From the data in Table 3, it can be seen that the Graded Transfer strategy performs best in improving model accuracy, especially in Sample Sets 1, 2, and 5, where the accuracy rate is significantly higher than the No Pre-training and Frozen Fine-tuning strategies, with increases of 7.33%, 2.82%, and 5.31%, respectively. In other sample sets, although the improvement with the Graded Transfer strategy is relatively smaller, it still outperforms the other strategies overall. This indicates that graded transfer learning, through progressive freezing and fine-tuning of network layers, can more effectively utilize the knowledge of pre-trained models, improving the model's generalization ability and detection performance. In contrast, while the Frozen Fine-tuning strategy also shows improvement, its enhancement in some sample sets is smaller, indicating that its utilization of pre-trained model knowledge is not as comprehensive as the Graded Transfer strategy. The No Pre-training strategy performs relatively poorly across all sample sets, further validating the importance of pre-training and transfer learning in enhancing model performance.

Table 4 shows the experimental results of the graded transfer strategy at different transfer stages. For Sample Set 1, the accuracy at the first stage transfer is 78.25%, at the second stage is 92.32%, and increases to 94.58% at the third stage. Sample Set 2's accuracy improves from 70.23% at the first stage to 98.59% at the second stage, and reaches 99.23% at the third stage. Sample Set 3 shows accuracy rates of 75.69%, 84.21%, and 93.51%. For Sample Set 4, the accuracy rates are 66.32%, 98.36%, and 98.26% at each stage. Sample Set 5's accuracy improves from 75.46% to 86.54%, and then to 96.25%. Sample Set 6 has accuracy rates of 75.23% at the first stage, 96.36% at the second stage, and 99.36% at the third stage. From the data in Table 4, it can be observed that the graded transfer strategy significantly improves model accuracy at each stage, with particularly notable improvements between the first and second stages. This indicates that the graded transfer strategy, by progressively freezing and fine-tuning network layers, allows the model to gradually adapt to new data distributions, thereby enhancing its generalization ability and detection performance. The accuracy in the first stage is relatively low, but after the second stage transfer, it significantly improves to a higher level, such as 98.59% for Sample Set 2 and 98.36% for Sample Set 4. The fine-tuning at the third stage further improves accuracy, although the increase is relatively small, overall performance is best, such as 99.36% for Sample Set 6.

Table 4. Experimental results of graded transfer strategy at different transfer stages

Sample Set Name	First Stage Transfer	Second Stage Transfer	Third Stage Transfer
Sample Set 1	78.25%	92.32%	94.58%
Sample Set 2	70.23%	98.59%	99.23%
Sample Set 3	75.69%	84.21%	93.51%
Sample Set 4	66.32%	98.36%	98.26%
Sample Set 5	75.46%	86.54%	96.25%
Sample Set 6	75.23%	96.36%	99.36%

5. CONCLUSION

This study focuses on the motor control systems of new energy vehicles, aiming to improve system performance and reliability through two main directions: adaptive signal filtering magnetic chain identification and motor health monitoring. In terms of magnetic chain identification, this paper proposes a method based on EKF, which effectively improves the accuracy of magnetic chain parameter estimation, thereby enhancing system control performance. Experimental results show that using this method for magnetic chain identification significantly reduces the current harmonics in the control system, verifying its effectiveness in motor control optimization. For motor health monitoring, this paper introduces a graded transfer learning strategy, which enhances the model's generalization ability by progressively freezing and fine-tuning network layers. Experimental results indicate that the graded transfer strategy significantly improves the detection accuracy of sample sets at different transfer stages, particularly excelling in health monitoring of new energy vehicle motor control systems. Compared to other transfer strategies, such as no pre-training and frozen fine-tuning, the graded transfer strategy shows clear advantages in accuracy and stability. This result demonstrates that the graded transfer strategy can better adapt to complex motor operating environments, providing more reliable technical support for fault detection.

The research presented in this paper holds significant value for the new energy vehicle industry by improving motor control system performance and reliability through enhanced magnetic chain identification methods and advanced transfer learning strategies. It achieves accurate magnetic chain identification and improves motor health monitoring accuracy, contributing to extending motor lifespan and enhancing overall safety of new energy vehicles. However, the study also has some limitations. Firstly, in the practical application of the EKF method, the choice of model parameters has a significant impact on system performance and needs further optimization and adjustment. Secondly, although the graded transfer learning strategy performs well in this study, its generalization ability in more complex and dynamically changing real-world conditions still requires further validation. Future research could address these limitations by: 1) investigating parameter optimization issues for EKF to enhance its adaptability under different operating conditions; 2) exploring more complex transfer learning models and algorithms to improve model generalization and robustness in dynamic conditions. Additionally, applying the research findings to more types of motors and control systems could validate their universality and practical application value. These efforts will further advance new energy vehicle motor control technology, improving system intelligence and operational efficiency.

ACKNOWLEDGEMENT

This paper was supported by General Topic of Teaching Reform Research of Vocational Education and Adult Education in Jilin Province in 2024 (Grant No.: 2024ZCY251).

REFERENCES

[1] Zhi, J., Wang, X., Shi, Q., Yao, Z., Qi, Y. (2023). Torque allocation strategy based on economy and stability for electric vehicle considering controllability after motors failure. Proceedings of the Institution of Mechanical Engineers, Part D: Journal of Automobile Engineering, 237(12): 2759-2779. https://doi.org/10.1177/09544070221121838

[2] Zhao, Y., Wang, M., Wang, K. (2020). Application of photoelectric sensor in vehicle power control system. Journal of Nanoelectronics and Optoelectronics, 15(6): 700-706. https://doi.org/10.1166/jno.2020.2794

[3] Schlimme, H.C., Henze, R. (2023). Brake-by-wire system redundancy concept for the double point of failure scenario. SAE International Journal of Vehicle Dynamics, Stability, and NVH, 7(3): 329-341. https://doi.org/10.4271/10-07-03-0021

[4] Mohammadi Pirouz, H., Hajizadeh, A. (2020). A highly reliable propulsion system with onboard uninterruptible power supply for train application: Topology and control. Sustainability, 12(10): 3943. https://doi.org/10.3390/su12103943

[5] Shang, Y., Li, X., Qian, H., Wu, S., Pan, Q., Huang, L., Jiao, Z. (2019). A novel electro hydrostatic actuator system with energy recovery module for more electric aircraft. IEEE Transactions on Industrial Electronics, 67(4): 2991-2999. https://doi.org/10.1109/TIE.2019.2905834

[6] Ou, C., Pan, F., Lin, S. (2024). Cascade failure-based identification and resilience of critical nodes in automotive supply chain networks. Sustainability, 16(13): 5514. https://doi.org/10.3390/su16135514

[7] Song, H., Dong, M., Wang, X. (2024). Research on inertial force attenuation structure and semi-active control of regenerative suspension. Applied Sciences, 14(6): 2314. https://doi.org/10.3390/app14062314

[8] Bennbaia, S., Mahdi, E., Abdella, G., Dean, A. (2023). Composite plastic hybrid for automotive front bumper beam. Journal of Composites Science, 7(4): 162. https://doi.org/10.3390/jcs7040162

[9] Gorelik, K., Kilic, A., Obermaisser, R. (2019). Connected energy management system for automated electric vehicles with fail-operational powertrain and powernet. IEEE Transactions on Vehicular Technology, 68(10): 9588-9603. https://doi.org/10.1109/TVT.2019.2934777

[10] Kilic, A. (2021). New fail operational powernet methods and topologies for automated drivingwith electric vehicle. Turkish Journal of Electrical Engineering and Computer Sciences, 29(2): 1092-1105. https://doi.org/10.3906/elk-2005-14

[11] Ramana, T.V., Manaktala, S.S., Valarmathi, K., Doohan, N.V., Shetty, D.K., Kumar, H., Akwafo, R. (2022). Energy auditing in three-phase brushless dc motor drive output for electrical vehicle communication using machine learning technique. Wireless Communications

and Mobile Computing, 2022(1): 9644795. https://doi.org/10.1155/2022/9644795
[12] Cao, X., Yang, W., Yao, Y. (2019). Electric car design based on wheel motor drive. IOP Conference Series: Materials Science and Engineering, 573(1): 012074. https://doi.org/10.1088/1757-899X/573/1/012074
[13] Ye, W., Liu, Y., Wu, G., et al. (2022). Design optimization and manufacture of permanent magnet synchronous motor for new energy vehicle. Energy Reports, 8: 631-641. https://doi.org/10.1016/j.egyr.2022.10.136
[14] Popescu, L., Craiu, O. (2023). Energy consumption analysis for an EV powertrain using three BLDC identical motors. Revue Roumaine des Sciences Techniques—Série Électrotechnique et Énergétique, 68(2): 152-157. https://doi.org/10.59277/RRST-EE.2023.68.2.6
[15] Godfrey, A.J., Sankaranarayanan, V. (2018). A new electric braking system with energy regeneration for a BLDC motor driven electric vehicle. Engineering Science and Technology, An International Journal, 21(4): 704-713. https://doi.org/10.1016/j.jestch.2018.05.003
[16] Nguyen, C.T., Nguyễn, B.H., Ta, M.C., Trovão, J.P.F. (2023). Dual-motor dual-source high performance EV: A comprehensive review. Energies, 16(20): 7048. https://doi.org/10.3390/en16207048
[17] Park, H.J., Lim, M.S. (2019). Design of high power density and high efficiency wound-field synchronous motor for electric vehicle traction. IEEE Access, 7: 46677-46685. https://doi.org/10.1109/ACCESS.2019.2907800
[18] Hua, M., Chen, G., Zhang, B., Huang, Y. (2019). A hierarchical energy efficiency optimization control strategy for distributed drive electric vehicles. Proceedings of the Institution of Mechanical Engineers, Part D: Journal of Automobile Engineering, 233(3): 605-621. https://doi.org/10.1177/0954407017751788
[19] Adnane, M., Nguyen, C.T., Khoumsi, A., Trovão, J.P.F. (2024). Real-time torque-distribution for dual-motor off-road vehicle using machine learning approach. IEEE Transactions on Vehicular Technology, 73(4): 4567-4577. https://doi.org/10.1109/TVT.2024.3355186
[20] Kim, H.J., Lee, C.S. (2021). Shape parameters design for improving energy efficiency of IPM traction motor for EV. IEEE Transactions on Vehicular Technology, 70(7): 6662-6673. https://doi.org/10.1109/TVT.2021.3089576